Title TBD

Author List TBD

1 Introduction

Observations of slow-slip and low-frequency earthquakes in nature suggest that fault failure encompasses a spectrum of slip modes [9, 5, 2]. While the explanations for non-traditional earthquakes remain a topic of debate, they have been observed in many subduction zones, including Cascadia [**?**, **?**], Mexico [**?**], Costa Rica [**?**], Japan [**?**], and New Zealand [**?**]. What causes strain energy to be released across a wide-range of failure behaviors is not understood, and is made more difficult by the limited methods of observation on natural faults. Laboratory stick-slip is often used to model and study repeating earthquake behavior [3, 6]. Frictional stability of a system is predicted to bifurcate at a critical stiffness , k_c [4]. For systems in which $k > k_c$, linearly stable response is exptected, while systems with $k < k_c$ are dynamically unstable [10]. Behavior at and near k_c is not well understood, but transitional behaviors such as sinusoidal stress variations and slow-slip have been observed [7, 1, 8] Here we show that critical stiffness is not a fixed parameter, but evolves with shearing until the material is pushed through a transitory region of condition stability into traditional fast, stick-slip behavior. We demonstrate stable, slow-slip, and stick-slip behavior in the laboratory by modifying the aggregate shear stiffness of the system.

2 Main

Biaxial double-direct shearing experiments were performed with humidified Min-U-Sil® simulated fault gouge. Force and displacement are recorded on both axes, as well as a measurement of the shearing block position (Fig.1). System compliance can be modified by changing the normal stress (2,4,6,8,12 MPa) or the material of which the shearing block is made (steel or cast acrylic).

System stiffness measured in cycles of unloading and reloading the shear stress provide an estimate of aggregate stiffness for all experiments regardless of failure behavior. Stiffnesses recovered from the loading portion of individual stick-slip events show very low stiffnesses during early frictional oscillations and emerging slow-slip due to the non-static nature of the system. These values of "working stiffness" do not represent the overall stiffness of the system, but a stiffness influenced by continued slip and creep. As dynamic failure reaches a steady state, we see agreement between the two methods of stiffness measurement (Fig.**??**).

Experiments performed under stiff system conditions exhibited linearly-stable behavior in response to order of magnitude velocity perturbations. Linearly-stable response is characterized by direct matching of the loading and system velocities and a transitory frictional response. Experiments of identical conditions, but in a more compliant system exhibited emergent unstable behavior, beginning with frictional oscillations, and transitioning to dynamic frictional failure. Oscillations and

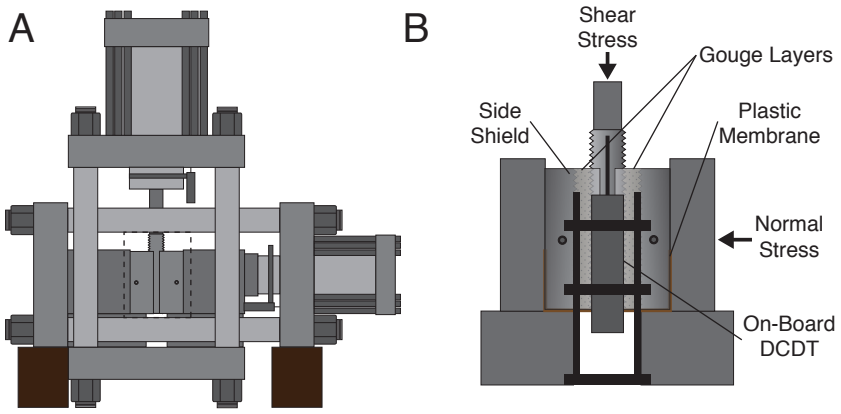

Figure 1: The biaxial deformation apparatus (A) and sample configuration (B). Two large hydraulic pistons are servo-controlled in either force or displacement control modes. Double direct shear samples are supported by steel blocks. Samples use metal side shields and a plastic membrane to reduce gouge extrusion. Local displacement transducers (DCDTs) can be referenced to the center block to avoid apparatus stiffness corrections and measure deformation of the center block.

dynamic failure are characterized by relatively rapid accelerations and decelerations of the system above/below the load point velocity when the material yields under excessive shear force. Experiments with further increased compliance exhibited very rapid dynamic failure that was audible and classified as fast stick-slip.

For experiments exhibiting stable sliding behavior, velocity steps were imposed to obtain the rate-and-state frictional parameters of the material and system. The rate-and-state parameters are constants to an emperical fit to transient response of a frictional system to a perturbation [**?**]. The a parameter provides a measure of the direct effect in response to a velocity step, and b provides the magnitude of friction evolution there-after. The difference of a and b, then yields a quantitative measure of how strongly velocity strengthening or velocity weakening a material is. The critical slip distance, D_c, is often considered to be the slip required to renew the contact population in a granular material. In our experiments, a remains relatively constant with displacement, but b evolves asymptotically upwards with increasing shear displacement. During this transitional period, the critical slip distance evolves downwards (Fig.2).

The transition from velocity strengthening to velocity weakening and corresponding decrease in k_c increase the value of the predicted critical stiffness (eq.1). When the critical stiffness intersects the measured system stiffness, we begin to see frictional oscillations and dynamic failure. The larger the departure from $k = kc$, the more dramatic the behavior. Very stiff systems show no tendency to produced damped oscillations after a velocity step. Very compliant systems exhibit fast dynamic failure. (Fig. 3)

$$k_c = \frac{b - a}{D_c} \tag{1}$$

There are two conditions for unstable behavior to occur: 1) that the material be velocity neutral to velocity weakening, and 2) that the system stiffness be at or below the critical stiffness [**?**, 10]. Velocity weakening is a necessary, but insufficient condition for unstable behavior. If a material is velocity strengthening, any acceleration leading to slip is immediately arrested by increased shearing

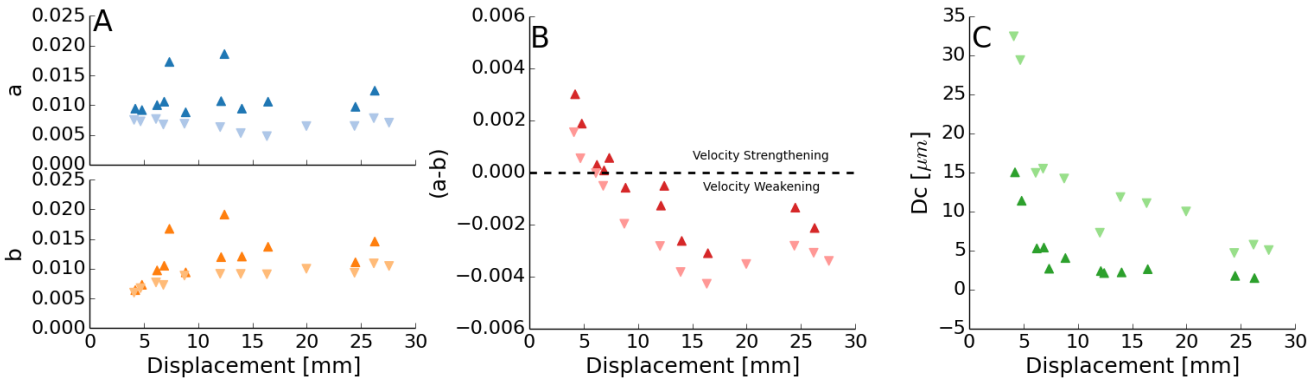

Figure 2: Rate-and-state friction parameters obtained from velocity step inversions. All inversions were accomplished with a fixed stiffness of 5.5x10$^{-3}\mu$m. A) rate-and-state parameter a remains relatively constant with displacement and shows a systematic behavior with higher values of a always being observed during velocity up-steps. The b parameter shows a similar behavior, but also increases with displacement, reaching a steady-state value around 10 mm displacement. B) The sample transitions from velocity strengthening to velocity weakening behavior at around 10 mm and remains velocity weakening for the remainder of the experiment. C) Critical slip distance estimates show considerable scatter, but do reduce to a steady-state value of 5-10 um.

resistance and the energy is frictionally dissipated. The stiffness of the system governs the rate at which energy stored as strain can be released. If the energy release occurs in such a way that the drop in shear resistance with displacement occurs faster than the drop in applied shearing force with displacement, the system can support unstable failure.

Increases in measured aggregate system stiffness from layer compaction due to grain rearrangement, layer thinning with increased shear strain, possible grain comminution and increased packing, localization of shear, and reduction of compliant center block material above sample due to geometric effects with shear. Layer compaction due to rearrangement and geometric thinning with shear have been well documented [**?**]. At these low stresses, grain comminution is minimal. Shear localization effects does play a role in the evolution of layer behavior [**?**]. The reduction in the amount of compliant center block material above the shearing zone with accumulated displacement is minimal compared to these other effects.

Our observations of transitional behavior beginning when $k \sim k_c$ suggests that k_c is a valid proxy for the stability of a system, marking a transitory zone between stable sliding and stick-slip that encompasses slow-slip and oscillatory behavior. We also observe that the critical stiffness of a system evolves with shear strain, suggesting that tectonic faults may change behavior as they accumulate slip and become mature fault zones.

Laboratory results can also be connected to observations in nature through the critical patch size. Critical patch size (eq.2) grows with increasing k_c and/or increasing normal stress. Extending this to large patch sizes hypothesized for slow-slip events suggests lowered normal stress, possibly due to high pore-pressures and/or low critical stiffness values.

$$r_c = \frac{16}{7\pi} G \frac{D_c}{\sigma_n (b-a)} \tag{2}$$

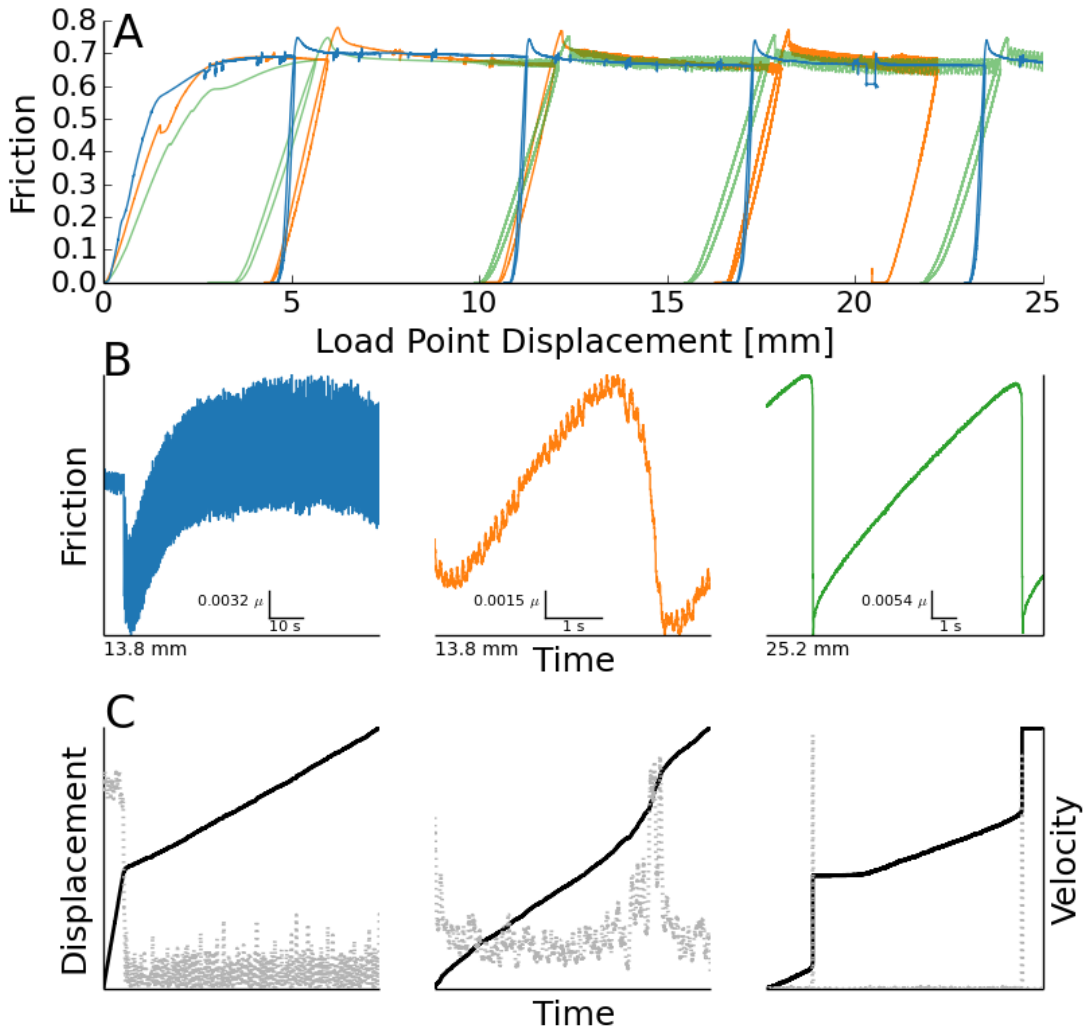

Figure 3: A) Run-plots of experiments p4309 (blue), p4311 (orange), and p4316 (green). Different working stiffnesses can be observed as the slope of unload/reload segments. B) All steel blocks produced stable responses to velocity steps (left). Destiffening the system with an acrylic center block produced non-audible slow-slip events (center). Further destiffening with an acrylic center block and increased normal stress produced audible fast stick-slip events(right). C) Center block displacement (black) and velocity (gray) for the corresponding types of failure.

3 Methods

All experiments were performed on a servo-controlled biaxial shearing apparatus. Displacements on the normal and shearing axes were measured by Direct Current Displacement Transducers (DCDTs) referenced at the end-platens and ram nose. The displacement of the shearing block was measured with a DCDT referenced at the end-platen and the top of the shearing block. Loads applied to the sample were measured with strain gauge load cells. All transducers are semi-annually calibrated with a traceable transfer standard.

Samples were prepared in the double-direct-shear geometry using steel or titanium side blocks and steel or acrylic shearing blocks. All blocks were grooved 0.8 mm deep at 1 mm spacing to reduce boundary effects. The sample area was 10 x 10 cm and filled with Min-U-Sil to a thickness of 3 mm. Granular layers were left in a sealed container overnight with a solution of anhydrous sodium carbonate to humidify the samples.

After samples were loaded into the load frame, a constant normal stress was applied and maintained by the servo system in a force feedback control mode. Samples were allowed to compact and accomodate grain rearrangement before shearing began. Shearing is conducted at a fixed rate in displacement feedback control mode.

Stiffness of the system was altered by changing the applied normal stress and by changing the material of the shearing block. Increasing normal stress decreases the effective stiffness of the system, as does switching the steel forcing block for a cast acrylic block.

Layers were built of Min-U-Sil® 40 fine ground silica from the U.S. Silica® company Berkeley Springs, West Virginia plant. The median diameter of grain is 10.5 μm. The product is 99.5 % SiO_s, with traces of metal oxides making up the remainder.

System stiffnesses from unload/reload shear stress cycles were calculated by a least-squares linear fit in friction vs. displacement for the interval $\mu = 0.3 - 0.4$. Stiffnesses from the loading portion of slow-slip and stick-slip events were obtained with a derivative based algorithm [8]. Rate-and-state models were fit with both the Dieterich and Ruina laws, with comparable results. Inversions were done with an iterative singular value decomposition technique.

References

[1] T. Baumberger, F. Heslot, and B. Perrin. Crossover from creep to inertial motion in friction dynamics. *Nature*, 367(6463):544–546, 1994.

[2] Gregory C. Beroza and Satoshi Ide. Slow earthquakes and nonvolcanic tremor. *Annual Review of Earth and Planetary Sciences*, 39(1):271–296, 5 2011.

[3] W. F. Brace and J. D. Byerlee. Stick-slip as a mechanism for earthquakes. *Science*, 153(3739):990–992, 1966.

[4] Ji-Cheng Gu, James R Rice, Andy L Ruina, and Simon T Tse. Slip motion and stability of a single degree of freedom elastic system with rate and state dependent friction. *Journal of the Mechanics and Physics of Solids*, 32(3):167–196, 1984.

[5] Satoshi Ide, Gregory C. Beroza, David R. Shelly, and Takahiko Uchide. A scaling law for slow earthquakes. *Nature*, 447(7140):76–9, 5 2007.

[6] P. A. Johnson, B. Ferdowsi, B. M. Kaproth, M. Scuderi, M. Griffa, J. Carmeliet, R. A. Guyer, P-Y. Le Bas, D. T. Trugman, and C. Marone. Acoustic emission and microslip precursors to stick-slip failure in sheared granular material. *Geophysical Research Letters*, 40(21):5627–5631, 11 2013.

[7] Bryan M. Kaproth and C. Marone. Slow earthquakes, preseismic velocity changes, and the origin of slow frictional stick-slip. *Science*, 341(6151):1229–32, 9 2013.

[8] J.R. Leeman, M.M. Scuderi, C. Marone, and D.M. Saffer. Stiffness evolution of granular layers and the origin of repetitive, slow, stick-slip frictional sliding. *Granular Matter*, Submitted.

[9] Zhigang Peng and Joan Gomberg. An integrated perspective of the continuum between earthquakes and slow-slip phenomena. *Nature Geosci*, 3(9):599–607, 8 2010.

[10] Christopher H. Scholz. *The mechanics of earthquakes and faulting*. Cambridge university press, 2002.

4 Acknowledgements

The authors with to thank Steve Swavely for his support in the laboratory. This material is based upon work supported by the National Science Foundation under Grant No. DGE1255832. Any opinions, findings, and conclusions or recommendations expressed in this material are those of the author(s) and do not necessarily reflect the views of the National Science Foundation. The work was also supported by funds from the GDL Foundation and Shell Oil Company.

5 Author Contributions

All authors contributed to data interpretation, analysis schema, and writing. J. Leeman conducted experiments and data analysis.

6 Competing Financial Interests

The authors declare no competing financial interests. Supplementary information accompanies this paper on www.nature.com/naturegeoscience. All data is avaliable for download, as well as Python scripts/notebooks to replicate data analysis on GitHub (www.github.com/jrleeman). Reprints and permissions information is available online at http://npg.nature.com/reprintsandpermissions. Correspondence and requests for materials should be addressed to J. Leeman.